Legionella pneumophila inhibits macrophage apoptosis by targeting pro-death members of the Bcl2 protein family

Simran Banga*, Ping Gao*, Xihui Shen*, Valena Fiscus†, Wei-Xing Zong‡, Lingling Chen†, and Zhao-Qing Luo*§

*Department of Biological Sciences, Purdue University, 915 West State Street, West Lafayette, IN 47907; †Department of Biology, Indiana University, 915 East Third Street, Bloomington, IN 47405; and ‡Department of Molecular Genetics and Microbiology, Stony Brook University, Stony Brook, NY 11794

Edited by Frederick M. Ausubel, Harvard Medical School, Boston, MA, and approved January 30, 2007 (received for review December 12, 2006)

To establish a vacuole that supports bacterial replication, *Legionella pneumophila* translocates a large number of bacterial proteins into host cells via the Dot/Icm type IV secretion system. Functions of most of these translocated proteins are unknown, but recent investigations suggest their roles in modulating diverse host processes such as vesicle trafficking, autophagy, ubiquitination, and apoptosis. Cells infected by *L. pneumophila* exhibited resistance to apoptotic stimuli, but the bacterial protein directly involved in this process remained elusive. We show here that SidF, one substrate of the Dot/Icm transporter, is involved in the inhibition of infected cells from undergoing apoptosis to allow maximal bacterial multiplication. Permissive macrophages harboring a replicating *sidF* mutant are more apoptotic and more sensitive to staurosporine-induced cell death. Furthermore, cells expressing SidF are resistant to apoptosis stimuli. SidF contributes to apoptosis resistance in *L. pneumophila*-infected cells by specifically interacting with and neutralizing the effects of BNIP3 and Bcl-rambo, two proapoptotic members of Bcl2 protein family. Thus, inhibiting the functions of host pro-death proteins by translocated effectors constitutes a mechanism for *L. pneumophila* to protect host cells from apoptosis.

bacterial pathogenesis | type IV secretion | intracellular pathogen | cell death

Programmed cell death plays an important role in the defense against pathogens, and manipulation of host cell apoptotic processes could determine the outcome of the interplay between the host cell and a pathogen (1). Many pathogens have thus evolved various sophisticated strategies to manipulate the execution of programmed cell death pathways for successful colonization of the host. Among these, a variety of viruses code for proteins that specifically inhibit host apoptotic pathways to ensure maximal multiplication (1). Similarly, some bacterial pathogens such as *Chlamydia trachomatis* and *Bartonella henselae* suppress cell death in infected cells (2, 3).

Legionella pneumophila is a facultative intracellular pathogen capable of multiplying in a wide spectrum of eukaryotic cells. Intracellular growth of *L. pneumophila* requires the Dot/Icm type IV protein translocation system that injects a large number of bacterial effectors into host cells (4). These translocated bacterial proteins are believed to reorchestrate host cellular processes, thus allowing the vacuole containing internalized *L. pneumophila* to undergo a unique trafficking route that bypasses the endocytic pathways. By intercepting vesicles originating from the endoplasmic reticulum (ER), the *L. pneumophila*-containing vacuole eventually is transformed into a compartment characteristic of rough ER (5). Consistent with this notion, *L. pneumophila* modulates the activities of vesicle trafficking regulatory molecules such as small GTPases Arf1 and Rab1 by translocated guanine nucleotide exchange factors specific for these proteins, thus facilitating the acquisition of ER materials and the subsequent intracellular bacterial multiplication (6–8).

Modulation of nonvesicle trafficking pathways by *L. pneumophila* also is important for its intracellular replication; perturbation of the ER-associated degradation machinery by RNAi leads to repression of bacterial growth, suggesting that this pathogen exploits the proteasome-dependent protein degradation system (9). In mammalian cells, infection by *L. pneumophila* leads to the activation of two independent cell death pathways. In murine macrophages expressing a restrictive allele of *birc1e*, a gene encoding a member of the nucleotide binding oligomerization (NOD) proteins that sense the presence of intracellular invaders (10), infection of *L. pneumophila* leads to activation of caspase 1 and subsequent cell death (11). Recent studies indicated that activation of this caspase 1-dependent cell death pathway requires the bacterial flagellin protein as well as the Dot/Icm transporter (12, 13). In permissive macrophages, early studies suggested that *L. pneumophila* actively induces apoptosis via the activation of caspase 3 (14). However, recent studies indicate that vigorous bacterial replication did not lead to apoptosis in infected cells (15). Instead, macrophages harboring actively replicating *L. pneumophila* exhibit strong resistance to exogenous cell death stimuli (16). These observations indicate that an apoptotic process is initiated in macrophages in response to *L. pneumophila* infection and replication, but the bacteria are able to inhibit or reverse the process in a Dot/Icm-dependent manner, possibly by injecting effectors that can interfere with apoptotic pathways. Consistent with this hypothesis, two recent studies showed that a large number of antiapoptotic genes were induced in cells infected by virulent *L. pneumophila* strains via the activation of the multifunctional transcriptional regulator NF-κB (17, 18). Moreover, the Dot/Icm substrate SdhA was recently shown to be required for protecting macrophages from cell death by a yet-unknown mechanism (19). In this study we present evidence that the Dot/Icm system substrate SidF (20) is involved in inhibition of host cell death during *L. pneumophila* intracellular growth in permissive macrophages, at least in part by directly interacting with and neutralizing the activities of two pro-death members of the Bcl2 protein family.

Results

Permissive Macrophages Infected by a *sidF* Mutant Are More Apoptotic. After verifying Dot/Icm-mediated translocation of SidF into infected cells during infection [see supporting information (SI) Fig. 7],

Author contributions: S.B., P.G., X.S., and Z.-Q.L. designed research; S.B., P.G., X.S., V.F., and Z.-Q.L. performed research; W.-X.Z. and L.C. contributed new reagents/analytic tools; S.B., P.G., X.S., and Z.-Q.L. analyzed data; and Z.-Q.L. wrote the paper.

The authors declare no conflict of interest.

This article is a PNAS direct submission.

Abbreviations: ER, endoplasmic reticulum; MOI, multiplicity of infection.

§To whom correspondence should be addressed. E-mail: luoz@purdue.edu.

This article contains supporting information online at www.pnas.org/cgi/content/full/0611030104/DC1.

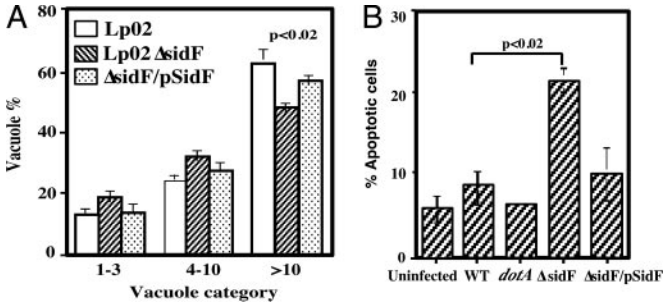

Fig. 1. Phenotypes associated with infection by the *sidF* mutant. (*A*) The *sidF* mutant formed fewer large phagosomes. Mouse macrophages were infected at an MOI of 1, and the distribution of vacuoles was determined at 14 h after infection as described (32). Strains tested are Lp02(intact *dot/icm*), Lp03(*dotA*$^-$) (data not shown), Lp02ΔsidF, and Lp02ΔsidF harboring pZL623(pSidF). Data are from two independent experiments performed in triplicate, and >150 vacuoles were scored in each sample. (*B*) Mouse macrophages infected with a *sidF* mutant are more apoptotic. Uninfected cells and cells infected with Lp02(*dot/icm* intact), Lp03(*dotA*$^-$), or Lp02(Δ*sidF*) and Lp02(Δ*sidF/pSidF*) for 14 h were fixed. Intracellular bacteria were labeled by indirect fluorescence staining with anti-*L. pneumophila* antibody, and the apoptotic status of the cells was probed by TUNEL staining. Samples were scored for fragmented chromatin by counting infected cells displaying positive TUNEL signals. Similar data were obtained from more than five independent experiments, and data from one representative experiment are shown.

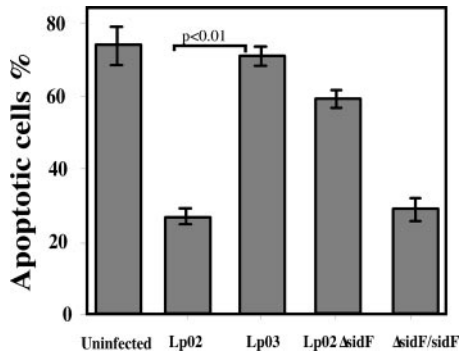

Fig. 2. SidF is important in apoptosis resistance exhibited in *L. pneumophila*-infected macrophages. Uninfected U937 or cells infected with Lp02(*dot/icm* intact), Lp03(*dotA*$^-$), Lp02(Δ*sidF*), or Lp02(Δ*sidF/pSidF*) at an MOI of 1 for 8 h were treated with 2 μM staurosporine for an additional 4 h. After fixation, bacterial vacuoles were labeled by immunostaining, and the morphology of cell nuclei was labeled with Hoechst staining. The apoptotic status of infected cells was scored by counting infected cells displaying fragmented nuclei. Data shown are averages of three independent experiments, with standard deviations.

we studied the function of SidF by analyzing a *sidF* mutant for several cell biological characteristics associated with vacuoles containing *L. pneumophila*. In murine bone marrow-derived macrophages the mutant was defective in intracellular growth, consistently exhibiting an ≈3-fold growth defect (SI Fig. 8). Consistent with this observation, in mouse macrophage the SidF mutant formed a significantly lower percentage of vacuoles containing >10 bacteria (Fig. 1*A*). No growth defect was detected in the human monocytic cell line U937 or in the amoeba host *Dictystelium discoideum* (SI Fig. 9*A* and data not shown). Despite its detectable intracellular growth defect in mouse macrophage, the *sidF* mutant still is able to efficiently avoid fusion with lysosome; it also can efficiently acquire ER proteins such as calnexin and Bip (data not shown). Thus, we asked whether SidF is involved in modulating host apoptotic pathways by examining the apoptotic status of cells infected with the *sidF* mutant. In mouse macrophages 1 h after infection, no difference was observed between uninfected cells and cells infected by any strains. In each case, <5% of the cells stained positively for apoptosis (data not shown). At the 14-h time point no change in the proportion of apoptotic cells was observed in samples infected by the *dotA* mutant Lp03, with <5% of the infected cells staining positively for apoptosis (Fig. 1*B*). Approximately 6% of cells infected with the wild-type strain Lp02 appeared apoptotic (Fig. 1*B*). However, ≈22% of the cells infected by the *sidF* mutant were apoptotic at this time point, significantly higher than that of cells infected by the wild-type strain ($P < 0.02$) (Fig. 1*B*). The apoptosis rate of cells infected by the *sidF* mutant can be partially suppressed by introducing a plasmid carrying the *sidF* gene (Fig. 1*B*). The incomplete complementation most likely results from overexpression of SidF from the high-copy plasmid (SI Fig. 7), probably by interfering with the translocation of apoptosis-inducing effectors. Such an increased cell death rate also was observed in U937 cells (SI Fig. 9*B*). Taken together, these data suggest that SidF is involved in the inhibition of host cell apoptosis during infection.

SidF Contributes to Cell Death Resistance in Macrophages Infected by Wild-Type *L. pneumophila*. Macrophages harboring replicating *L. pneumophila* exhibit resistance to apoptosis stimuli (16). To examine whether SidF contributes to such resistance, we infected U937 cells with *L. pneumophila* and subsequently treated these cells with staurosporine for 4 h. The apoptotic status of infected cells was examined by Hoechst staining followed by microscopic inspection. In samples infected for 2 h, 4 h of staurosporine treatment resulted in extensive cell death in all samples, with ≈80% of the infected cells appearing apoptotic (data not shown). In samples that had been infected for 8 h, ≈78% of the cells infected by the *dotA* mutant were apoptotic, a rate similar to the 82% observed in the uninfected samples (Fig. 2). Consistent with earlier studies (16), cells infected by the wild-type strain were resistant to this cell death stimulus, with only ≈26% of the cells being apoptotic (Fig. 2). However, the ratio of apoptotic cells in the *sidF* mutant infection is ≈58%, a value significantly higher than that of cells infected by the wild type ($P < 0.01$) (Fig. 2). Furthermore, expression of SidF from a plasmid in the mutant fully restored resistance to staurosporine, with ≈28% of the infected cells being apoptotic (Fig. 2). Similar results were obtained when infection was allowed to proceed for 10 h before adding staurosporine (data not shown). These data further suggested a role of SidF in apoptosis resistance conferred by cells harboring replicating *L. pneumophila*.

Mammalian Cells Expressing SidF Are Resistant to Staurosporine-Induced Apoptosis. The above observations strongly suggested that SidF is directly involved in blocking apoptosis in cells infected by virulent *L. pneumophila*. To further demonstrate the cell death inhibition activity of SidF, we transduced two different cell lines with adenoviral particles containing a SidF expression construct and examined whether cells expressing SidF confer resistance to apoptosis stimuli. Twenty-four hours after transduction, we treated the cells with 1 μM staurosporine and examined cell death by nuclear staining. In HeLa cells this agent induced apoptosis in most control cells transduced with a virus containing vector DNA, with ≈68%, 88%, and 95% of the cells being apoptotic after drug treatment for 3.5, 7, and 10 h, respectively (Fig. 3 *C–E*). In contrast, many SidF-expressing cells survived, with only 31%, 36%, and 46% of the cells having succumbed to the drug (Fig. 3 *A*, *B*, and *E*).

In U937 cells transduced with control vector viruses, drug treatment for 3.5 h resulted in ≈49% apoptosis, whereas only 24% of the cells transduced to express SidF were apoptotic. Extending drug treatment to 7 and 10 h led to more extensive apoptotic cells death in cells not expressing SidF, with ≈68% and 96% showing apoptotic nuclear morphology, respectively (Fig. 3*B*). In samples

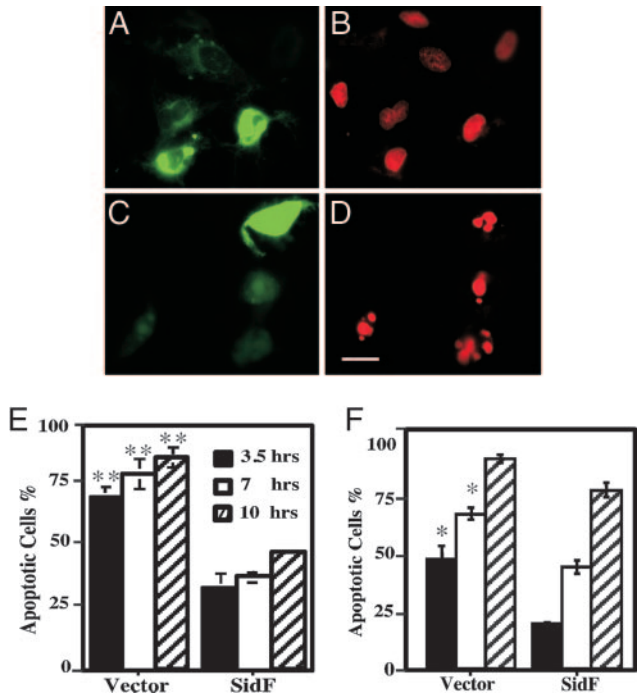

Fig. 3. Cells expressing SidF are resistant to apoptosis induced by staurosporine. HeLa cells were transduced with adenovirus particles harboring a construct directing expression of a GFP::SidF chimera (*A* and *B*) or GFP (*C* and *D*) for 24 h before being treated with 1 μM staurosporine for 7 h. The nuclear morphology was visualized by Hoechst 33342 staining (pseudocolored in red for ease in distinguishing) (*B* and *D*). (Scale bar: 20 μm.) (*E* and *F*) Kinetic analysis of apoptotic status of the HeLa cells (*E*) and U937 cells (*F*). Transduced cells treated with 1 μM staurosporine for 3.5, 7, and 10 h were fixed, stained, and scored for the rates of apoptosis. Data shown are one representative of at least three independent experiments performed in triplicate, with at least 350 cells inspected for each sample. *, $P < 0.05$; **, $P < 0.01$.

transduced to express SidF, such incubation times caused significantly less apoptosis, with ≈46% and 72% of the cells displaying condensed nuclei ($P < 0.01$) (Fig. 3*B*). Taken together, these data revealed that cells expressing SidF exhibited strong resistance to cell death insults. Moreover, the increased apoptotic rates after prolonged drug treatment indicated that SidF does not completely block staurosporine-induced apoptosis, but rather delays the onset of cell death, particularly in U937 cells.

SidF Interacts with BNIP3 and Bcl-rambo, Two Pro-Death Members of the Bcl2 Protein Family. SidF is not homologous to any known protein, making it difficult to understand the molecular mechanisms of its cell death inhibition activity and the importance of such activities in the intracellular replication of *L. pneumophila*. Thus, we set up a yeast two-hybrid screening to identify host proteins that specifically interact with SidF. Analysis of clones appearing on selective medium led to the identification of several proteins, including BNIP3 and Bcl-rambo, two proteins belonging to the Bcl2 protein family as putative binding targets of SidF (SI Table 1) (21, 22). Given the cell death related observations discussed above, we chose to focus on BNIP3 and Bcl-rambo. In the cDNA clone harboring BNIP3, the activation domain (AD) of GAL4 was fused to the 42nd residue of the target with an intact C terminus. In the case of Bcl-rambo, the fusion occurred at residue 296 of the 485-residue protein and the chimera also contains an intact C terminus. Reconstructed AD::BNIP3 and AD::Bcl-rambo fusions showed similar specific interactions with SidF in a yeast two-hybrid assay (Fig. 4*A*).

To substantiate the interactions seen between SidF and these two pro-death Bcl2 proteins in the yeast two-hybrid assay, we determined whether SidF could form complexes with these two proteins in mammalian cells. First, we expressed SidF and FLAG-tagged BNIP3 in 293T cells, lysed the cells with Nonidet P-40 and immunoprecipitated possible SidF/BNIP3 complexes with anti-SidF antibody. As shown in Fig. 4*B*, BNIP3 was present in immunoprecipitates only when SidF was coexpressed. The migration pattern of BNIP3 is similar to that previously reported, consisting of three bands of ≈60 kDa (dimer), 30 kDa, and 22 kDa (monomer) (23). No signals were detected in untransfected samples or in samples transfected with plasmids expressing only BNIP3 or SidF, indicating that the interactions were specific. Reciprocal experiments using the anti-FLAG antibody also specifically precipitated SidF (data not shown). These results indicated that SidF forms a protein complex with BNIP3 in mammalian cells.

We also analyzed interactions between SidF and Bcl-rambo. First, we coexpressed SidF and FLAG-tagged Bcl-rambo and analyzed precipitates using anti-SidF antibody; interactions between Flag-Bcl-rambo and SidF can be readily detected (Fig. 4*D*). Second, we analyzed whether SidF interacts with endogenous Bcl-rambo. We first prepared a Bcl-rambo-specific antibody with a recombinant protein (see *Materials and Methods*). This antibody specifically recognized Bcl-rambo expressed in several cell lines in a pattern similar to that described earlier (data not shown and ref. 21). We then transfected 293T cells with a plasmid expressing SidF or the empty vector and prepared precipitates with our anti-Bcl-rambo antibody; SidF was detected not only in precipitates from cells transfected to overexpress Bcl-rambo, but also in cells transfected with the control vector (Fig. 4*E*), indicating that SidF forms a complex with endogenous Bcl-rambo (Fig. 4*E*). Furthermore, the amount of SidF detected from cells expressing exogenous Bcl-rambo was considerably higher than that from vector-transfected cells (Fig. 4*E*).

We further examined interactions between SidF and Bcl-rambo under infection condition. To this end, lysates of U937 cells infected with relevant *L. pneumophila* strains at a multiplicity of infection (MOI) of 5 for 6 h were analyzed. Immunoprecipitates were prepared by using anti-Bcl-rambo antibody, and the presence of SidF in the precipitates was probed. Although SidF was not detected in precipitates from cells infected with the wild-type strain Lp02, we were able to detect this protein in immunoprecipitates obtained from cells infected with the SidF overexpressing strain (Fig. 4*F*). As expected, no SidF was detected in total lysates of cells infected with the Dot/Icm-deficient strain Lp03 overexpressing SidF or the *sidF* deletion mutant (Fig. 4*F*). The failure to detect protein complex formed by SidF and Bcl-rambo in cells infected with wild-type bacteria most likely is due to the low abundance of SidF injected into those cells by this bacterial strain (Fig. 4*F*, input). This observation is consistent with our SidF immunostaining data in which almost all phagosomes containing this SidF-overexpressing strain stained positively for this protein (SI Fig. 7). The association of SidF with Bcl-rambo in infected cells further strengthened our conclusion that Bcl-rambo is one target of SidF.

We next established an *in vitro* assay to analyze whether SidF directly binds Bcl-rambo. Despite a predicted hydrophobic domain in its carboxyl terminus, we found that a portion of bacterially expressed GST-Bcl-rambo was soluble in PBS buffer, and thus we have affinity-purified this protein to ≈90% purity (Fig. 4*G*). We performed a pull-down experiment by incubating purified SidF with glutathione-resin or resin coated with the GST-Bcl-rambo or GST. After extensive washes, we found that SidF was retained only by resin coated with GST-Bcl-rambo (Fig. 4*H*), indicating that SidF directly binds Bcl-rambo and that the interactions between these two proteins can occur after they have properly folded.

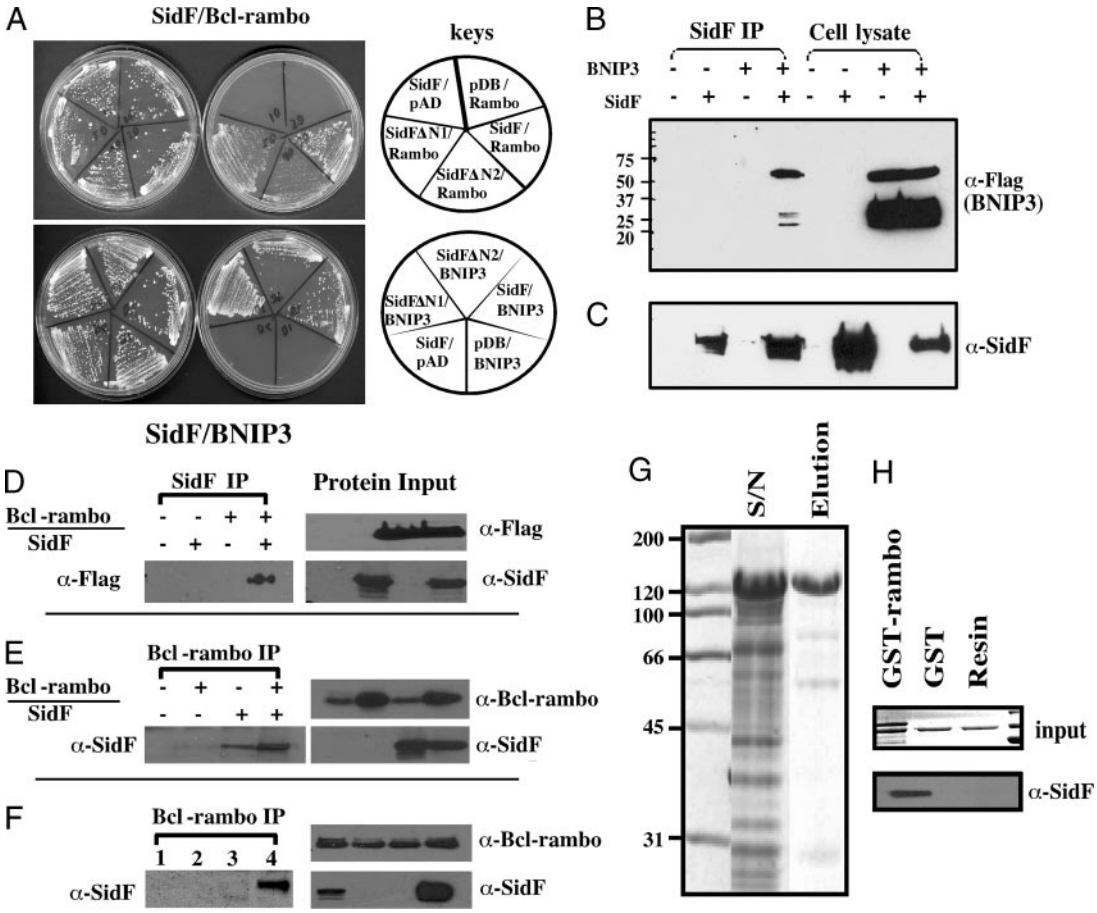

Fig. 4. SidF interacts with BNIP3 and Bcl-rambo. (*A*) Interactions between SidF and Bcl2-rambo/BNIP3 in yeast two-hybrid assay. Yeast strains harboring the indicated constructs were streaked on Leu$^-$ and Trp$^-$ synthetic medium to select for plasmids (on the left) or on Leu$^-$, Trp$^-$, Ade$^-$, and His$^-$ medium to examine the interactions (on the right). The two SidF deletion mutants tested were SidFΔN1, SidF250–912 and SidFΔN2, SidF650–912. (*B*) SidF forms complexes with BNIP3. Cell lysates of 293T cells transfected with the indicated plasmid combinations were analyzed either directly or after immunoprecipitation by immunoblots with an anti-FLAG antibody. Relevant molecular mass markers are shown on the left in kilodaltons. (*C*) SidF in total cell lysates was detected by anti-SidF antibody. (*D–F*) SidF interacts with Bcl-rambo in mammalian cells. (*D*) 293T cells were transfected with the indicated plasmid combinations, and cell lysates were used for immunoprecipitation. Flag-Bcl-rambo was detected with an anti-FLAG antibody. (*E*) SidF forms a complex with endogenous Bcl-rambo. SidF was probed in immunoprecipitates obtained with anti-Bcl-rambo antibody from cells transfected with shown plasmid combinations. Note that more SidF was detected in precipitates of cells transfected with a Bcl-rambo-expressing plasmid. (*F*) SidF and Bcl-rambo form a complex in cells infected by a Dot/Icm-competent strain overexpressing SidF. Lysates of U937 cells infected with wild-type (lane 1), dotA$^-$(pSidF) (lane 2), the *sidF*$^-$ mutant (lane 3), or ΔsidF(pSidF) (lane 4) for 6 h were subjected to immunoprecipitation with anti-Bcl-rambo antibody, and the presence of SidF/Bcl-rambo complexes was probed with anti-SidF antibody. (*G* and *H*) SidF directly binds Bcl-rambo. (*G*) Purification of GST-Bcl-rambo. Relevant molecular mass markers are shown on the left in kDa. (*H*) Binding between Bcl-rambo and SidF. Glutathione beads or beads coated with GST or GST-Bcl-rambo were incubated with SidF for 4 h at 4°C. After extensive washing, bound proteins were eluted with SDS loading buffer, resolved by SDS/PAGE, and probed with anti-SidF antibody (*Lower*). Ten percent of input proteins were detected by Coomassie bright blue staining (*Upper*).

SidF Inhibits Cell Death Induced by Bcl-rambo. A common feature for antiapoptotic proteins that target pro-death proteins is their ability to inhibit cell death induced by their counterparts (24). Our observation that cells expressing SidF are resistant to cell death stimuli and that SidF specifically interacts with BNIP3 and Bcl-rambo suggested that SidF is able to protect cell death induced by these proteins. Thus, we cotransfected MCF-7 cells with constructs expressing SidF and Bcl-rambo. Twenty-four hours after transfection, cells were fixed and assessed for apoptosis by staining with Hoechst 33342. In cells transfected with vector DNA or cells transfected to express only SidF, <18% of the cells appeared apoptotic (Fig. 5). As expected, in samples transfected to express Bcl-rambo, >50% of the cells are apoptotic (Fig. 5). In cells transfected to express both Bcl-rambo and SidF, the rate of apoptotic cells decreased to ≈27%, significantly lower than samples expressing only Bcl-rambo ($P < 0.05$) (Fig. 5). These results indicated that SidF is able to inhibit cell death induced by Bcl-rambo, further establishing the role of SidF in preventing cell death.

A Domain Localized to the C-Terminal Half of SidF Is Important for Its Activity. Induction of apoptosis by pro-death members of the Bcl2 family in part is by titrating its pro-survival counterparts via the formation of heteromultimers through the BH motif (24). Because SidF does not contain any detectable BH domain, we defined its target-binding domains by deletion analysis. In yeast two-hybrid analysis, we found that a SidF mutant lacking as many as 750 aa from its N terminus still strongly interacts with Bcl-rambo and BNIP3 (Fig. 4*A* and data not shown). In mammalian cells, these mutants are still able to form complexes with Bcl-rambo (Fig. 6*A*). Furthermore, the cell death inhibition activity of the SidFΔN250 mutant was indistinguishable from that of the full-length SidF (Fig. 6*C*). However, loss of >650 aa from the N terminus of SidF resulted in mutants that no longer are able to inhibit activity of Bcl-rambo (Fig. 6*C*).

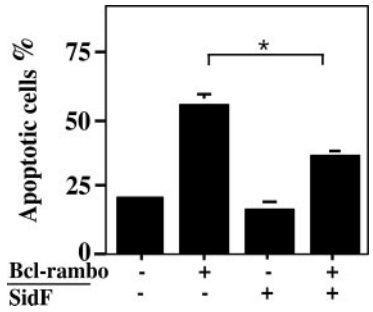

Fig. 5. SidF inhibits apoptosis induced by Bcl-rambo. MCF-7 cells were transfected with the indicated plasmid combinations for 24 h, and fixed cells were stained with Hoechst 33342 and scored microscopically for apoptotic nuclei. Data shown are from three independent experiments performed in triplicate; at least 200 transfected cells were scored for each sample. Cells transfected with both plasmids were identified by a GFP signal carried on the vector used to express SidF. *, $P < 0.05$.

On the other hand, mutants lacking 50 or 100 aa from the carboxyl terminus of SidF had considerably lost their ability to inhibit Bcl-rambo, although these mutants still detectably interact with Bcl-rambo (Fig. 6 *B* and *C*). Deletion of 150 residues from this end of SidF completely abolished both the target binding and inhibitory activity (Fig. 6 *B* and *C*). SidF contains two predicted 22-residue hydrophobic domains that are important for targeting the protein to the ER/nuclear regions (SI Fig. 10). Loss of a single hydrophobic domain drastically reduced its ability to interact with Bcl-rambo, whereas deletion of both such domains abolished its Bcl-rambo binding activity (Fig. 6*B*). In agreement with the loss of target binding activity, none of these mutants retained the ability to inhibit the activity of Bcl-rambo (Fig. 6*C*). Taken together, these results indicated that a carboxyl domain of SidF is important for target binding, but inhibition of apoptosis required a larger region extending to the central portion of the protein. The two putative hydrophobic domains may be directly involved in target binding or may be required for proper folding of SidF and thus subsequent target binding activity. Interestingly, the location of this functional domain is similar to the BID domain of BepA, a *B. henselae* protein that inhibits apoptosis by inducing cAMP production (3).

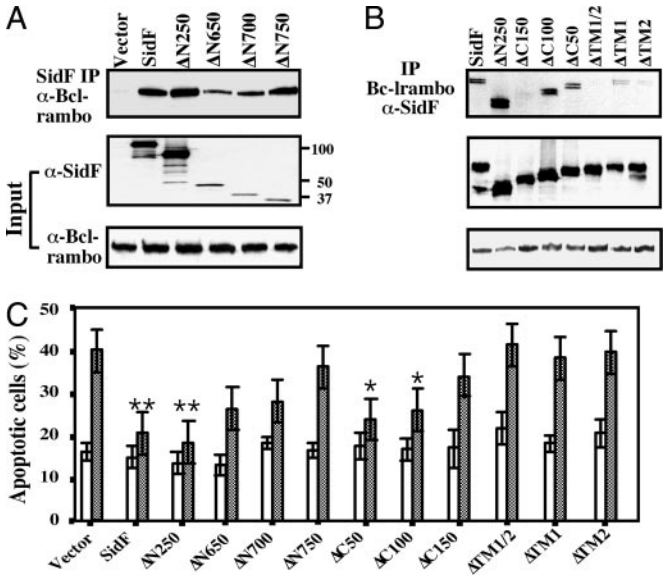

Fig. 6. The C-terminal portion of SidF is important for its activity. (*A* and *B*) Interactions between Bcl-rambo and SidF mutants. 293T cells were transfected with combinations of plasmids expressing Flag-Bcl-rambo and individual mutants. Precipitates were prepared with anti-SidF antibody (*A*) or with anti-Bcl-rambo antibody (*B*). The presence of target proteins was detected with appropriate antibodies. In each case, 5% of the lysate used for coimmunoprecipitation was probed for levels of input proteins in total cell lysates. (*C*) Inhibition of Bcl-rambo activity by SidF and its derivatives. MCF-7 cells were transfected to express SidF and its derivatives along with Bcl-rambo (shaded bars) or the vector (open bars). Twenty-four hours after transfection, cells were fixed and stained with Hoechst 33342 and apoptotic rates were scored. Data shown are from three independent experiments, with standard deviations. *, $P < 0.05$; **, $P < 0.01$.

Discussion

It is well established that *L. pneumophila* actively modulates host apoptotic pathways. Such modulation can occur at the transcriptional level because infection by *L. pneumophila* leads to the induction of several antiapoptotic genes via the activation of an NF-κB-dependent pathway (17, 18). Transcription of a number of pro-death genes, including the BH-3-only protein BNIP3 and many caspases, also was elevated in response to intracellular growth of the bacterium (17). The induction of pro-death genes poses a problem for infected cells because these proteins sensitize cells to environmental insults, which, during *L. pneumophila* infection, can be represented by intracellular growth of the bacterium or the translocation of toxic substrates into host cells (19). Here we present evidence that the bacterial protein SidF interferes with host cell death by directly interacting with and inhibiting activities of apoptotic proteins.

Several lines of evidence indicate that binding of SidF to its targets is highly specific. First, these proteins were identified multiple times independently in our original yeast two-hybrid screening (SI Table 1); second, binding of SidF to Bcl-rambo can be detected under various conditions, including in cells in which SidF is delivered directly from the bacterium (Fig. 4*F*); third, SidF did not detectably interact with several other pro-death proteins structurally similar to BNIP3 and Bcl-rambo (data not shown). Clearly, binding to the targets is not sufficient for SidF to exert its activities because N-terminal deletion mutants of SidF lacking >650 residues were still able to bind Bcl-rambo efficiently but failed to confer protection (Fig. 6 *A* and *C*). How elements not directly involved in target binding contribute to the cell death inhibitory activity remains to be determined.

SidF appears to play a role in preventing cell death by abolishing the activities of BNIP3 and Bcl-rambo. Formation of heterodimers between proapoptotic and antiapoptotic members of the Bcl2 protein family determines at least in part the susceptibility of cells to death signals (24). The mechanism of action of SidF seems similar to that of the cell-death inhibiting 19-kDa protein from adenovirus which inhibits activities of multiple pro-death proteins by direct binding (22). Differing from *C. trachomatis*, which causes degradation of a number of pro-death BH3-only proteins (25), infection of *L. pneumophila* did not lead to destabilization of either BNIP3 or Bcl-rambo (data not shown). Although both BNIP3 and Bcl-rambo contain a carboxyl transmembrane domain important for mitochondria targeting and for cell death induction, their mechanisms of action are different (21, 26). BNIP3 forms heterodimers with pro-survival members of the Bcl2 protein family such as Bcl2 and Bcl-X_L (26), but Bcl-rambo does not detectably interact with any pro-survival members of the Bcl2 protein family (21). Further analysis of how SidF exerts its activity will likely shed light on the mechanisms of action of these host proteins.

The function of SidF appears similar to that of the cell death protection protein SdhA (19). However, unlike the mild growth defect observed in the *sidF* mutant, loss of SdhA resulted in a severe growth defect accompanied by drastic morphological changes in the infected cells (19). SdhA seems to control pathways critical for maintaining the integrity of infected cells,

whereas SidF appears to function downstream of SdhA by targeting branched death pathways triggered by *L. pneumophila* infection. Thus, *L. pneumophila* is able to manipulate the apoptotic status of infected cells at different levels, ranging from controlling some major pathways to inhibition of specific pro-death proteins.

Protozoan is believed to be the natural host of *L. pneumophila* and infection of mammalian cells was considered to be accidental (27). Amoeba does not code for classic apoptotic pathways, or for proteins such as BNIP3 and Bcl-rambo. Given that BNIP1, a pro-death BH3-only protein of the BNIP3 family is involved in membrane fusion in the ER (28), it will be interesting to determine whether either BNIP3 or Bcl-rambo possesses similar dual functions and whether SidF interferes with such activities. Alternatively, in the light of our results and recent discoveries that *L. pneumophila* manipulates several functions specific to higher organisms, a mammalian host may have been a driving force in the evolution of this bacterium.

Materials and Methods

Bacterial Strains, Media, and Plasmid Construction. All *L. pneumophila* strains used in this study were derivatives of the Philadelphia 1 strain Lp02 (29). Details for manipulations of bacterial strains, primers, and construction of plasmids are described in *SI Materials and Methods* and in SI Tables 2 and 3.

Yeast Manipulation and Two-Hybrid Assay. Yeast strains were grown in YPD medium or in appropriate amino acid dropout minimal media. The *sidF* gene was fused to the activation domain of the Gal4 activator on pGBKT7 (SI Table 2). Yeast strain PJ-64A (30) was used for two-hybrid screening against the human cDNA library according to instructions of the manufacturer (BD Biosciences, San Jose, CA).

Cell Culture and Transfection. U937 cells were cultured and differentiated following standard protocols (31). Other cell lines, including 293T, HeLa, MCF-7, and COS1, were cultured in DMEM supplemented with 10% FBS. Cells grown to ≈80% confluence were transfected with Lipofectamine 2000 (Invitrogen, Carlsbad, CA) following the manufacturer's instructions. For experiments designed to assess the apoptosis inhibitory activity of SidF, to ensure high efficiency of cotransfection, a molar ratio of 1:3 (Bacl-rambo:SidF) of DNA was used. Mouse macrophages were prepared by using a published protocol (32) and were plated at 2×10^5 cells per well for infection.

Immunoprecipitation. We seeded 293T cells on 100-mm plates at 5×10^5 cells per plate 1 day before transfection and then transiently transfected cells with combinations of plasmids. In all experiments the total amount of plasmid DNA was kept constant by adding appropriate amounts of vector DNA. Proteins of interest were detected by Western blot after SDS/PAGE. For coimmunoprecipitation from lysates of infected cells, 5×10^7 U937 cells were infected at an MOI of 5 for 6 h with the indicated *L. pneumophila* strains. Cell lysis buffer and the details of immunoprecipitation are given in *SI Materials and Methods*.

Recombinant Adenoviral Particle Preparation and Transduction. *sidF* was cloned into the shuttle plasmid pCMV-YFP, and a recombinant adenoviral vector containing *sidF* was obtained through *in vivo* homologous recombination by using the Adeasy system (Stratagene). The primary stock was propagated four times in AD-293 cells to achieve titers of 10^{10} to 10^{12} infectious particles per milliliter. This viral suspension was used to transduce HeLa or U937 cells at an MOI of 10.

Cell Death Assays. The apoptotic status of mammalian cells was determined by the TUNEL assay with the *in situ* cell death detection kit TMR red (Roche, Indianapolis, IN) or by staining of nuclei with Hoechst 33342. Cell death was determined by scoring cells with positively labeled fragmented chromatin (TUNEL assay) or condensed nuclei (Hoechst staining). The rates of apoptotic cells obtained by TUNEL staining or by Hoechst staining are very similar.

Protein Purification, Antibodies, Immunostaining, and Western Blot. Details of protein purification, sources of antibodies, and concentrations of antibodies in each experiment are described in *SI Materials and Methods*.

We thank Drs. R. Isberg (Tufts Medical School, Boston, MA) and J. Tschopp (University of Lausanne, Lausanne, Switzerland) for reagents and Dr. Art Aronson and Ms. Virginia Livingston for critical reading of the manuscript. This work was supported by American Heart Association Grant 0535451Z (to Z.-Q.L.), National Institutes of Health Grants R01AI069344 (to Z.-Q.L.) and R01GM065260 (to L.C.), and a Collaboration in Life Sciences and Informatics Research pilot grant between Purdue University and Indiana University (to Z.-Q.L. and L.C.).

1. Creagh EM, Conroy H, Martin SJ (2003) *Immunol Rev* 193:10–21.
2. Fan T, Lu H, Hu H, Shi L, McClarty GA, Nance DM, Greenberg AH, Zhong G (1998) *J Exp Med* 187:487–496.
3. Schmid MC, Scheidegger F, Dehio M, Balmelle-Devaux N, Schulein R, Guye P, Chennakesava CS, Biedermann B, Dehio C (2006) *PLoS Pathog* 2:e115.
4. Bruggemann H, Cazalet C, Buchrieser C (2006) *Curr Opin Microbiol* 9:86–94.
5. Roy CR, Tilney LG (2002) *J Cell Biol* 158:415–419.
6. Nagai H, Kagan JC, Zhu X, Kahn RA, Roy CR (2002) *Science* 295:679–682.
7. Machner MP, Isberg RR (2006) *Dev Cell* 11:47–56.
8. Murata T, Delprato A, Ingmundson A, Toomre DK, Lambright DG, Roy CR (2006) *Nat Cell Biol* 8:971–977.
9. Dorer MS, Kirton D, Bader JS, Isberg RR (2006) *PLoS Pathog* 2:e34.
10. Fortier A, Diez E, Gros P (2005) *Trends Microbiol* 13:328–335.
11. Zamboni DS, Kobayashi KS, Kohlsdorf T, Ogura Y, Long EM, Vance RE, Kuida K, Mariathasan S, Dixit VM, Flavell RA, *et al.* (2006) *Nat Immunol* 7:318–325.
12. Ren T, Zamboni DS, Roy CR, Dietrich WF, Vance RE (2006) *PLoS Pathog* 2:e18.
13. Molofsky AB, Byrne BG, Whitfield NN, Madigan CA, Fuse ET, Tateda K, Swanson MS (2006) *J Exp Med* 203:1093–1104.
14. Molmeret M, Zink SD, Han L, Abu-Zant A, Asari R, Bitar DM, Abu Kwaik Y (2004) *Cell Microbiol* 6:33–48.
15. Derre I, Isberg RR (2004) *Infect Immun* 72:6221–6229.
16. Abu-Zant A, Santic M, Molmeret M, Jones S, Helbig J, Abu Kwaik Y (2005) *Infect Immun* 73:5339–5349.
17. Abu-Zant A, Jones S, Asare R, Suttles J, Price C, Graham J, Kwaik YA (2007) *Cell Microbiol* 9:246–264.
18. Losick VP, Isberg RR (2006) *J Exp Med* 203:2177–2189.
19. Laguna RK, Creasey EA, Li Z, Valtz N, Isberg RR (2006) *Proc Natl Acad Sci USA* 103:18745–18750.
20. Luo ZQ, Isberg RR (2004) *Proc Natl Acad Sci USA* 101:841–846.
21. Kataoka T, Holler N, Micheau O, Martinon F, Tinel A, Hofmann K, Tschopp J (2001) *J Biol Chem* 276:19548–19554.
22. Boyd JM, Malstrom S, Subramanian T, Venkatesh LK, Schaeper U, Elangovan B, D'Sa-Eipper C, Chinnadurai G (1994) *Cell* 79:341–351.
23. Vande Velde C, Cizeau J, Dubik D, Alimonti J, Brown T, Israels S, Hakem R, Greenberg AH (2000) *Mol Cell Biol* 20:5454–5468.
24. Gross A, McDonnell JM, Korsmeyer SJ (1999) *Genes Dev* 13:1899–1911.
25. Dong F, Pirbhai M, Xiao Y, Zhong Y, Wu Y, Zhong G (2005) *Infect Immun* 73:1861–1864.
26. Ray R, Chen G, Vande Velde C, Cizeau J, Park JH, Reed JC, Gietz RD, Greenberg AH (2000) *J Biol Chem* 275:1439–1448.
27. Cianciotto NP, Fields BS (1992) *Proc Natl Acad Sci USA* 89:5188–5191.
28. Nakajima K, Hirose H, Taniguchi M, Kurashina H, Arasaki K, Nagahama M, Tani K, Yamamoto A, Tagaya M (2004) *EMBO J* 23:3216–3226.
29. Berger KH, Isberg RR (1993) *Mol Microbiol* 7:7–19.
30. James P, Halladay J, Craig EA (1996) *Genetics* 144:1425–1436.
31. Tilney LG, Harb OS, Connelly PS, Robinson CG, Roy CR (2001) *J Cell Sci* 114:4637–4650.
32. Conover GM, Derre I, Vogel JP, Isberg RR (2003) *Mol Microbiol* 48:305–321.